Electronic Supplementary Material (ESI) for Nanoscale.

CLEAN GRAPHENE INTERFACES BY SELECTIVE DRY TRANSFER FOR LARGE AREA SILICON INTEGRATION

S. R. Na[1†], S. Rahimi[2†], L. Tao[2], H. Chou[2], D. Akinwande[2], K.M. Liechti[1*]

[1]Department of Aerospace Engineering and Engineering Mechanics

Research Center for the Mechanics of Solids, Structures and Materials

[2]Department of Electrical and Computer Engineering

The University of Texas at Austin

Austin, Texas 78712

kml@mail.utexas.edu

[†] These authors (S. R. Na and S. Rahimi) contributed equally to this work.

* Corresponding Author

Submitted to

Nanoscale

September 2015

Delamination modes of the double cantilever beam specimen at different rates

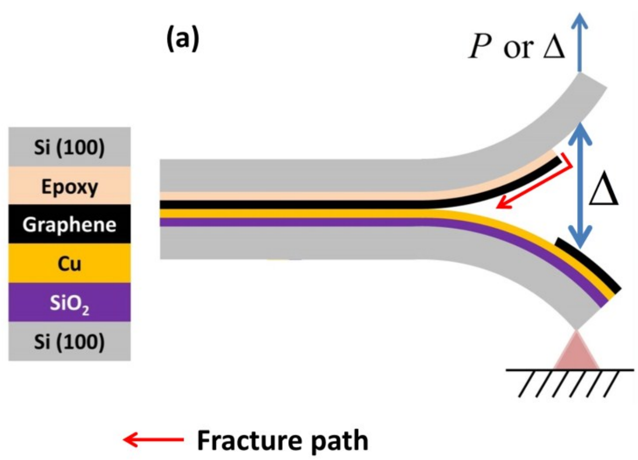

Figure S1. Delamination modes: (a) at 20 μm/s, the graphene/copper interface completely delaminated whereas (b) at 50 μm/s), the copper/silicon oxide interface completely delaminated.

Quality of graphene grown on copper film

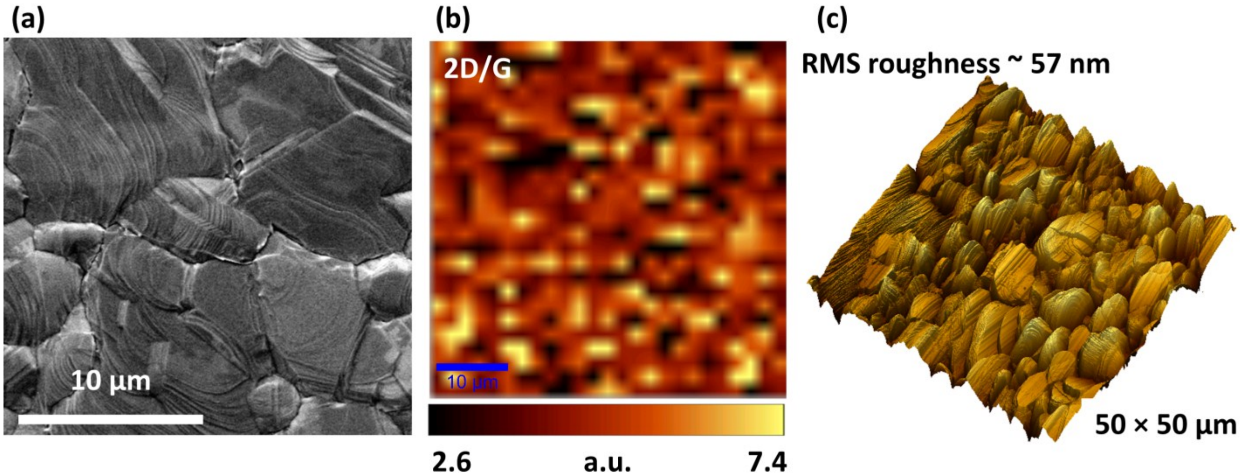

Figure S2. Surface characterization of graphene grown on copper film by CVD: (a) an SEM image of graphene on copper film, (b) Raman mapping data and (c) AFM scan over an area of 50 × 50 μm.

Fabrication of double cantilever beam samples

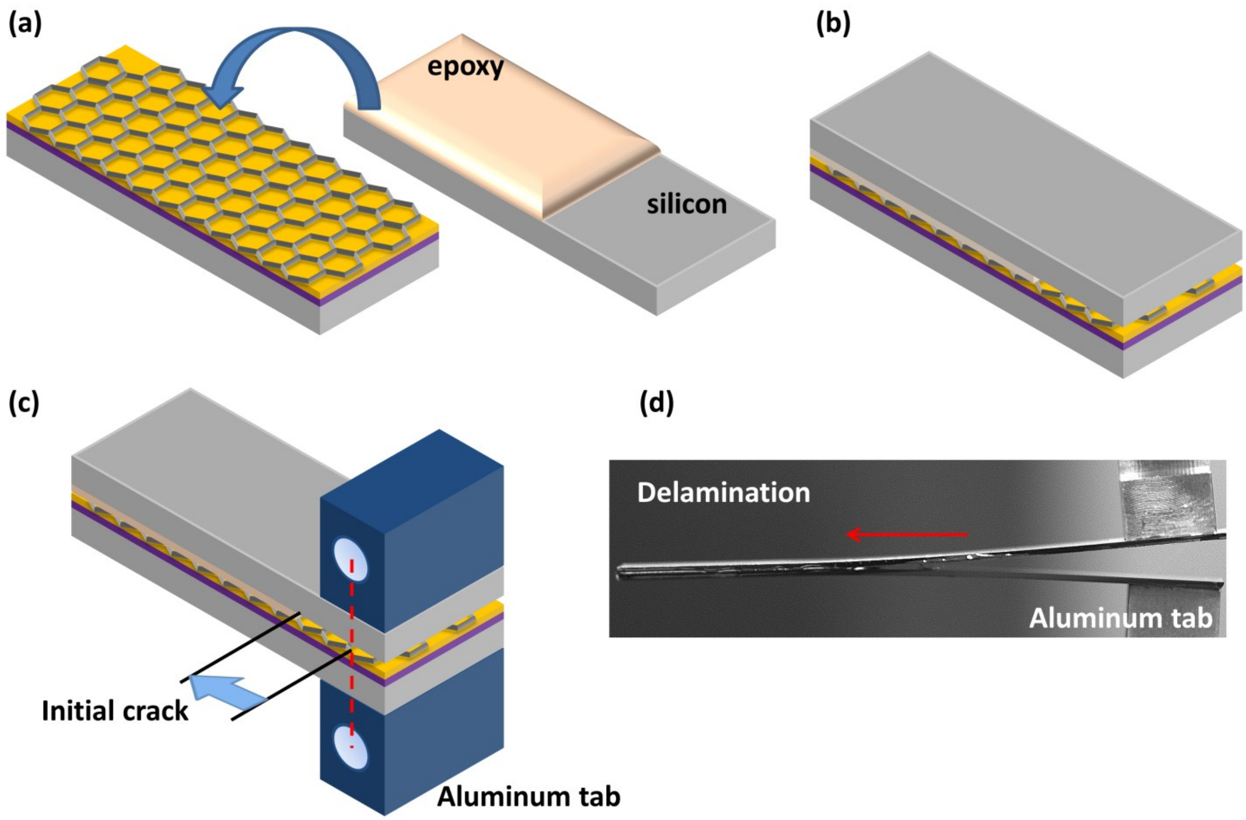

Figure S3. Schematic of the sample preparation

Once graphene was grown on copper film on thermally grown silicon oxide, degassed epoxy (EP30, Master Bond, Inc.) was partially spread over a second silicon strip (Fig. S3a), which was placed on the graphene-coated surface of the first silicon strip. The Si/epoxy/graphene/Cu/SiO_2/Si assembly (Fig. S3b) was cured at 100 ˚C for two hours, following the manufacturer's recommendations. The cure process results in a pre-notch, which is approximately 1-2 cm long and behaves as an initial blunt crack. Finally, two aluminum loading tabs (Fig. S3c) were rigidly bonded to the silicon strips. Figure S3d is a snapshot of the DCB under load.

Finite element analysis

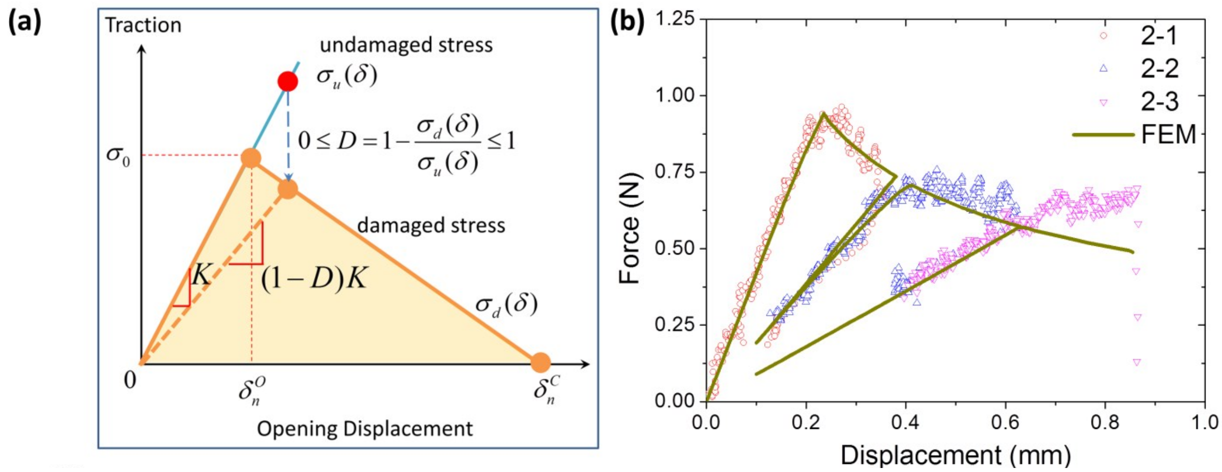

Figure S4. (a) Parameters associated with the bilinear traction-separation relation, (b) The measured force-displacement response at 50 μm/s (copper/silicon oxide delamination) is compared with the results of the simulation.

Although simple beam theory can be used to determine the adhesion energy, finite element analysis is required to determine the strength and the range of the adhesive interactions, which are embodied in traction-separation relations. The finite element analyses (FEM) were conducted with the commercial code ABAQUS 6.14®, which allows traction-separation relations, which are the continuum description of the adhesion interaction between two separate surfaces, to be modeled.

First, the thin copper film, silicon oxide and both Si (100) strips and the epoxy were modeled by four-node plain strain elements with reduced integration (CPE4R). The constitutive responses of silicon oxide and Si (100) were assumed to be homogeneous, isotropic and linearly elastic (Table S1) with moduli of 70 GPa and 129 GPa, respectively with the same Poisson's ratio of 0.23. The epoxy had a modulus of 3 GPa and Poisson's ratio of 0.45 with a plastic work-hardening model [1] to represent its inelastic behavior. The elastic-plastic behavior of the copper was determined by indenting copper film that had been grown on silicon and annealed from the same temperature that was used to grow the graphene. The Young's modulus and Poisson's ratio were 110 GPa 0.33, respectively. The copper yielded at 25 MPa and followed a linear hardening behavior with a stiffness of 3.33 MPa.

The analyses separately accounted for the interactions between graphene and copper or copper and silicon oxide through traction-separation relations (Fig. S4a) that yield the traction as:

$$\sigma = K_n \delta_n H\left(\delta_n^0 - \delta_n\right) + \left[1 - \frac{\delta_n^c\left(\delta_n - \delta_n^0\right)}{\delta_n\left(\delta_n^c - \delta_n^0\right)}\right] K_n \delta_n H\left(\delta_n - \delta_n^0\right), \tag{S1}$$

where K_n is the stiffness of the interaction prior to the onset of damage, δ_n is the separation, δ_n^0 is the value of the separation at which damage initiates, δ_n^c is the interaction range and $H\left(\delta_n\right)$ is the Heaviside function. The steady adhesion $\Gamma_{ss} = \frac{1}{2} K_n \delta_n^0 \delta_n^c$ is the area underneath the traction-separation relation. The values of the parameters for each interface are listed in Table 1.

Table S1. Material properties and thickness

	E (GPa)	σ_y (MPa)	ν	Thickness (μm)
Silicon oxide	70	N/A	0.23	520
Si(100)	129	N/A	0.23	0.35
Copper	110	25	0.35	0.3
Epoxy	3	40	0.45	

They were obtained by a parametric study where solutions for the load-displacement response were compared with the measured ones. It was necessary to reduce the strength and increase the interaction range in the traction-separation relations for the copper/silicon oxide interface to model the second and third loading cycles in the second sample. The first time the second sample was loaded, the crack grew from the bimaterial corner formed by the epoxy terminus and graphene, whereas the second and third loadings were applied to sharp cracks between the copper and silicon oxide, so the second traction-separation relation (TSR2) better represents the interaction between copper and silicon oxide.

Morphology of silicon oxide

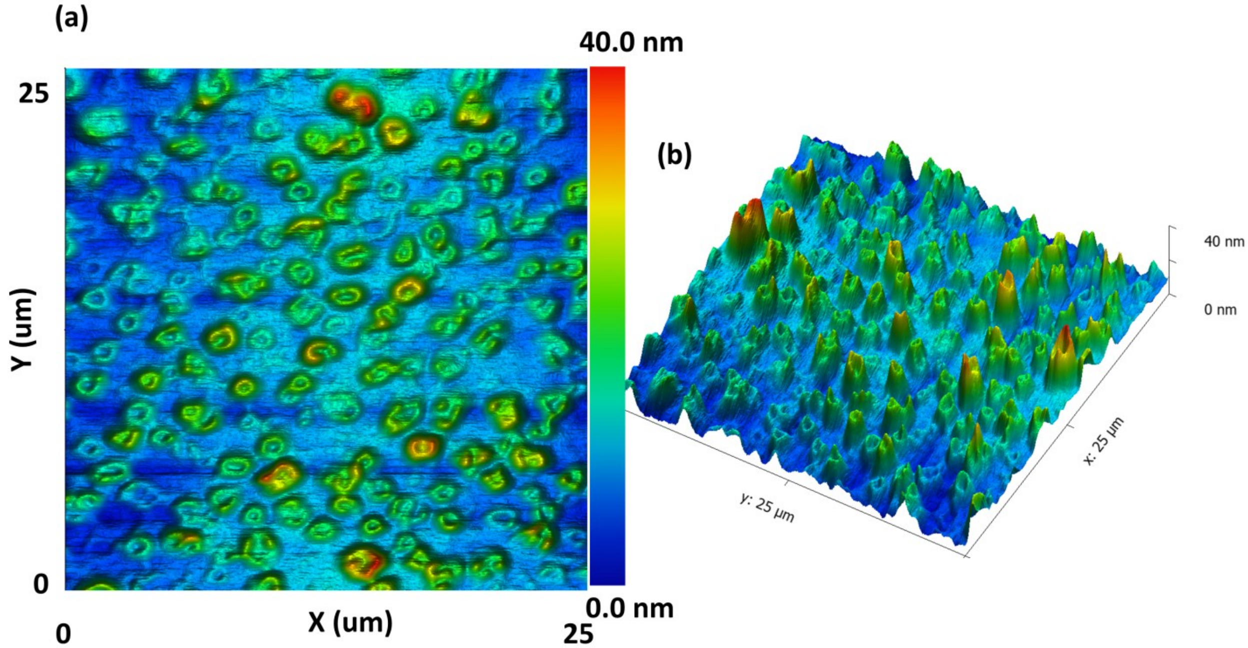

Figure S5. An AFM scan of the silicon oxide fracture surface following delamination along the interface between copper and silicon oxide at an applied displacement rate of 50 µm/s: (a) plan view and (b) three dimensional image of the fracture surface.

An applied displacement rate of 50 µm/s allowed both the graphene and its seed copper film to be completely transferred to the epoxy surface while exposing the silicon oxide surface. Surprisingly, AFM scanning of a 25×25-µm region exhibited interesting nanofeatures similar to calderas or volcanos on the silicon oxide surface. The RMS roughness of the scanned region was approximately 5.15 nm, a factor of 20 larger than mirror polished silicon surface. [1]

Bowker *et al.* [2] reported similar nanofeatures on silicon oxide surface during the formation of gold nanoparticles at high temperature (~1000 ˚C). The formation was related to the interaction of nanoparticles on the silicon oxide surface and oxidation of silicon at high temperature. It is possible that the approximately 900˚C temperature for graphene growth promotes similar interactions between copper and silicon oxide.

Morphology of graphene on copper and graphene on epoxy

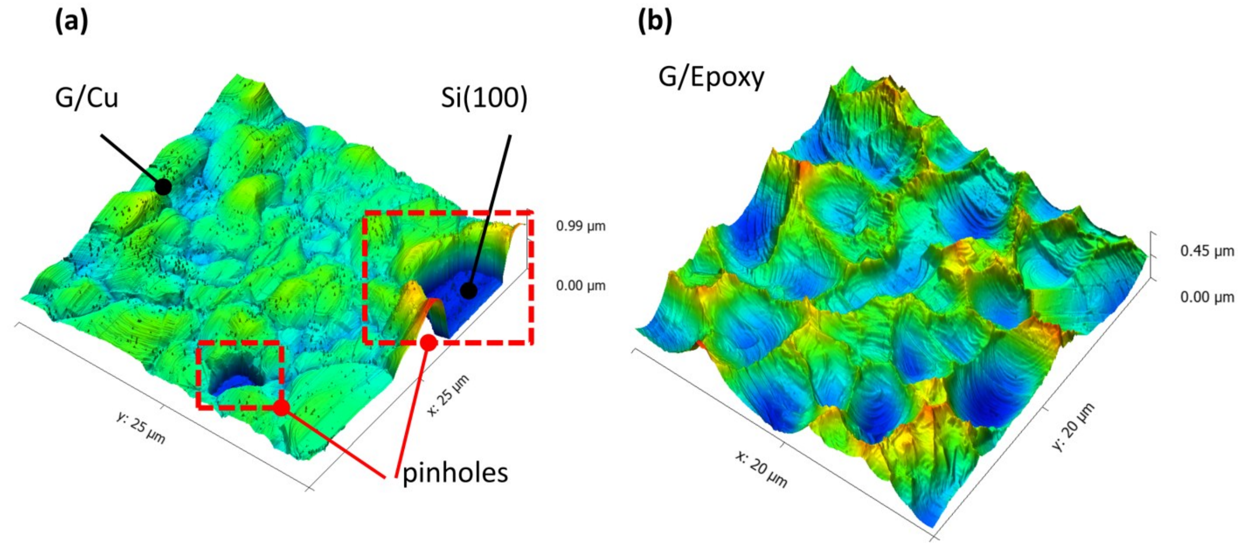

Figure S6. AFM scans of (a) graphene grown on copper film, and (b) graphene transferred to epoxy

High-resolution AFM scanning allowed us to obseve the morphologies of graphene on copper (Fig. S6a) following deposition and graphene on epoxy surface (Fig. S6b) after delamination at an applied displacement rate of 20 μm/s. From Figure S6a, it is possible to observe the characteristic features of the copper film following the deposition of graphene: steps within the copper grains, the copper grain boundaries, pinholes in the copper that expose the silicon oxide surface. The RMS roughness of the surface was approximately 70 nm, once the two pinholes were removed from the estimate.

An AFM scan of graphene transferred to epoxy following delamination along the graphene/copper interface (Fig. S6b) shows more details of the replicated morphology of the copper film. In the current experiment, the low viscosity epoxy replicated all the features of the copper film following the deposition of graphene. The estimated RMS roughness of the surface was approximately 74.3 nm, which is close enough the the value above to confirm that the low viscosity epoxy did indeed replicate such rough surface features.

Raman response of pure epoxy and graphene on epoxy

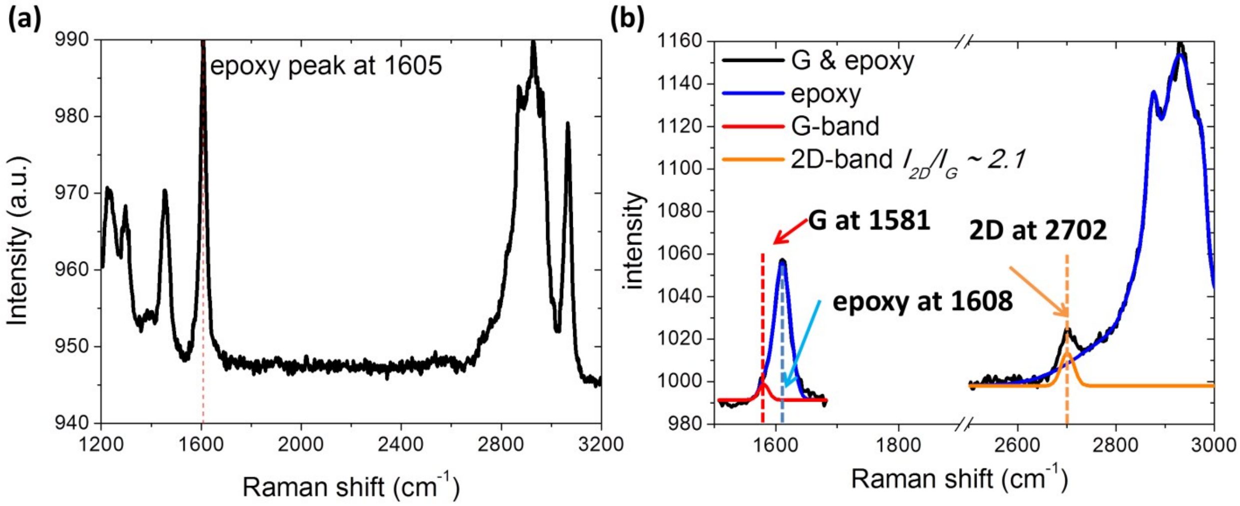

Figure S7. Raman response of (a) pure epoxy and (b) graphene transferred to epoxy.

Figure S7a exhibits the Raman response of pure epoxy, which has strong peak at 1605 cm^{-1}. Note the absence of peaks near 2700 cm^{-1} which are associated with location of the 2D band of graphene. Figure S7b shows the Raman response of graphene on epoxy (black), pure epoxy (blue) and the deconvoluted signals (red and orange) of graphene transferred to epoxy also shown in Figure 3d. The intensity ratio (I_{2D}/I_G) between the 2D (I_{2D}) and G bands (I_G) of graphene was approximately 2.1, indicating that the graphene was a monolayer of high quality (no D peak).

Procedures for device fabrication with transferred graphene or graphene/copper

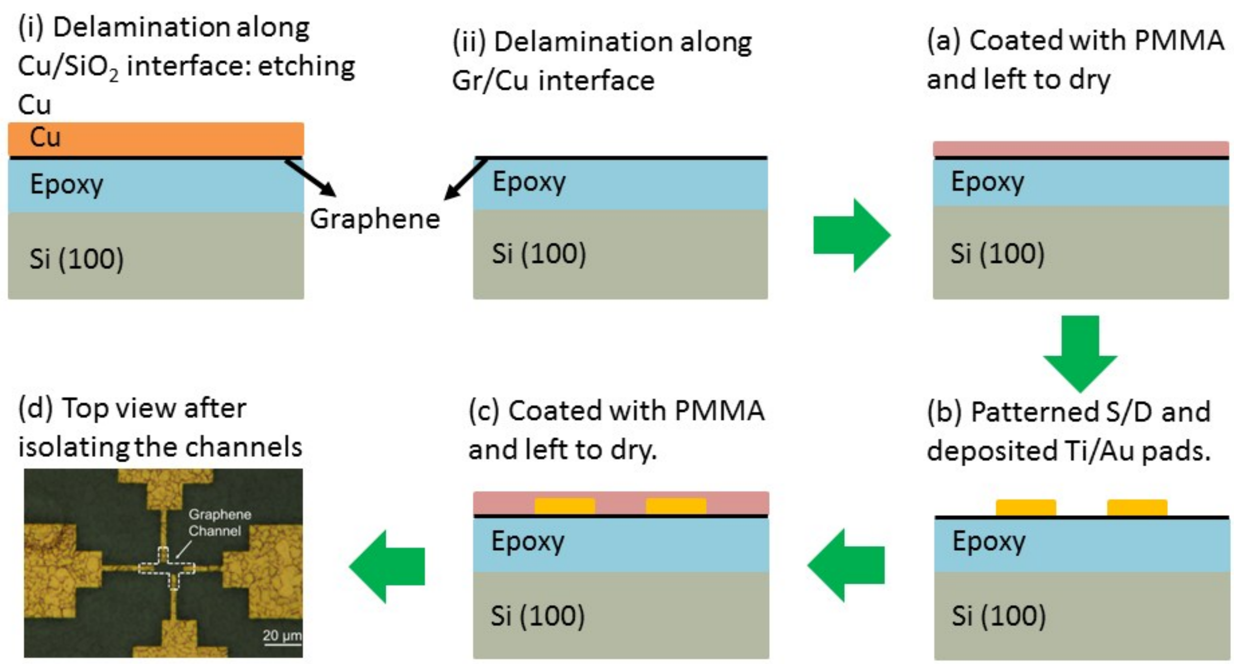

Figure S8. Schematic of the device fabrication process. In case (i), where copper/graphene was delaminated from the SiO2 substrate, the copper was etched in Ammonium per Sulfate (APS-100) solution before the device fabrication. The rest of the fabrication process is the same for both cases of (i) and (ii).

References

1. S. R. Na, J. W. Suk, R. S. Ruoff, R. Huang and K. M. Liechti, *ACS Nano*, 2014, **8**, 11234-11242.
2. M. Bowker, J. J. Crouch, A. F. Carley, P. R. Davies, D. J. Morgan, G. Lalev, S. Dimov and D.-T. Pham, *The Journal of Physical Chemistry C*, 2013, **117**, 21577-21582.